Dyes and Pigments 93 (2012) 1481–1487

Contents lists available at SciVerse ScienceDirect

Dyes and Pigments

journal homepage: www.elsevier.com/locate/dyepig

Synthesis, spectral properties of rhodanine complex merocyanine dyes as well as their effect on K562 leukemia cells

Jun-Feng Xiang [a], Yan-Xia Liu [a], Dan Sun [b], Su-Juan Zhang [b], Yi-Le Fu [a], Xiang-Han Zhang [a,c], Lan-Ying Wang [a,*]

[a] Key Laboratory of Synthetic and Natural Functional Molecule Chemistry, Ministry of Education, College of Chemistry and Materials Science, Northwest University, Xi'an 710069, PR China
[b] Institute of Photonics & Photon-Technology, Northwest University, Xi'an 710069, PR China
[c] School of Life Sciences and Technology, Xidian University, Xi'an 710071, PR China

ARTICLE INFO

Article history:
Received 10 August 2011
Received in revised form
21 October 2011
Accepted 30 October 2011
Available online 6 November 2011

Keywords:
Rhodanine complex merocyanine dyes
Spectral properties
DNA
BSA
Photosensitizers
Photodynamic therapy

ABSTRACT

Two rhodanine complex merocyanine dyes **9a** and **9b** were synthesized and their structures were confirmed by ^{1}H NMR, IR, MS, HRMS and UV–Vis spectra. From the spectral properties of the two dyes, it could be found that the λ_{max} of the dyes showed hypsochromic shifts with the increase of permittivity in protonic solvents, and bathochromic shifts with the increase of refractive index in non protonic solvents. The interactions of two dyes with DNA or BSA were also studied under physiological conditions. The results showed that the quantum yield of DNA-dye **9a** was up to 29.5 times compared with free dye **9a**. Dyes **9a** and **9b** were researched in Photodynamic Therapy (PDT) as well. It was demonstrated that supplementation of dye **9a** or **9b** as photosensitizers for PDT in K562 cells decreases the survival rate.

1. Introduction

It is well known that several approaches have been taken for cancer chemotherapy, and many antitumor drugs have been applied for clinic during the past 30 years. However, in the treatment of solid tumors the traditional approaches have met with only limited success and cancer still remains as one of the most serious diseases of human. Currently, in order to overcome the major drawbacks of chemotherapeutic antitumor drugs, e.g. adverse effects and drug resistance [1], photodynamic therapy (PDT) has attracted attention [2–6]. Besides chemotherapy, surgery, radiotherapy and immunotherapy, PDT is a promising therapeutic modality for the treatment of a variety of premalignant and malignant diseases [7]. Because of its low cytotoxicity, no surface damage, the capacity of highly selective and destroying tumors without harming normal tissues, PDT is a valuable therapy method.

Due to the strong fluorescence and absorption capacity, rhodanine merocyanine dyes, as derivatives of cyanine dyes, can be used as fluorescent labels for biomolecules [8–10]. Besides, they can distinguish some certain cells and selectively enter into cancer cells then kill it as photosensitizer directly using for PDT, or as a radiation sensitizer for the treatment of solid tumors [11]. In the meanwhile, this type of cyanine dyes used as antitumor drugs have been reported [12–17]. As the affinity between cyanine dyes and tumor cells is much higher than that between cyanine dyes and normal cells, combining PDT with drug therapy has become a tendency and will certainly promote the treatment of tumors. For this reason, we designed and synthetized two rhodanine complex merocyanine dyes **9a** and **9b** (Scheme. 1), and the products were confirmed by ^{1}H NMR, IR, MS, HRMS, UV–Vis. We studied the fluorescence and UV–Vis absorption spectra properties of two dyes in different solvents, and their interaction with DNA or BSA under physiological conditions. And using dye **9a** or **9b** as photosensitizers for PDT, its effect on K562 leukemia cells survival was analyzed.

2. Experimental

2.1. General

All reagents were obtained from commercial sources and used without further purification. The solvents were of analytical grade.

* Corresponding author. Tel.: +86 29 88302604; fax: +86 29 88303798.
E-mail address: wanglany@nwu.edu.cn (L.-Y. Wang).

0143-7208/$ – see front matter © 2011 Elsevier Ltd. All rights reserved.
doi:10.1016/j.dyepig.2011.10.017

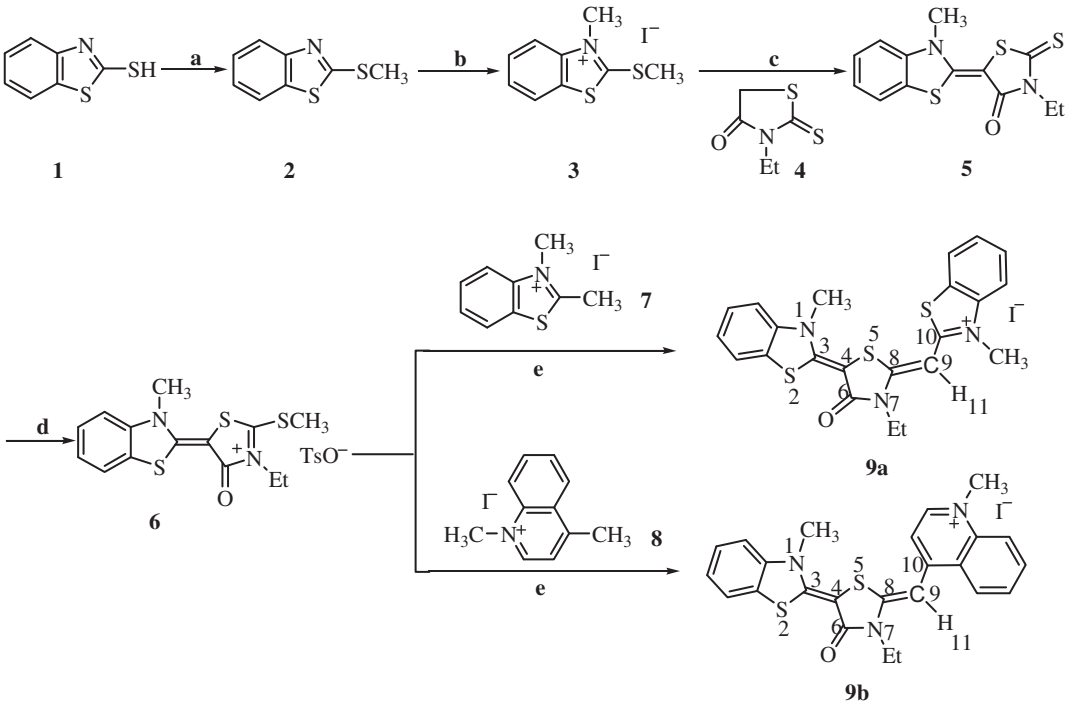

Scheme. 1. Reagents and conditions (a) $(CH_3)_2SO_4$, 10% NaOH, 40 °C (b) CH_3I, MeOH, 43 °C (c) Et_3N, EtOH, Reflux (d) TsOMe, DMF, 130 °C (e) Et_3N, MeCN, 70 °C.

Melting points were taken on an XT-4 micromelting apparatus and uncorrected. IR spectra in cm^{-1} were recorded on Shimadzu IR Prestige-21 spectrometer and Bruker Equiox-55 spectrometer. ^1H NMR spectra were recorded at 400 MHz on a Varian Inova-400 spectrometer and chemical shifts were reported relative to internal Me_4Si. The electron impact (EI) mass spectra were recorded at 70 eV with a GCMS-QP2010 system equipped with the solid sample direct insertion probe. HRMS was recorded on a microTOF-Q II ESI-Q-ToF LC/MS/spectrometer. The absorption spectra were recorded on a Purkinje General UV-1900 UV–Vis spectrometer. Fluorescence measurements were carried out on a Hitachi F-4500 spectrofluorimeter.

2.2. Preparation of the intermediate **2**–**8**

2-Methylthiobenzothiazole (**2**) [18], 3-methyl-2-methylthiobenzothiazolium iodide (**3**) [19], 5-(3-methyl-(3*H*)-benzothiazol-2-ylidene)-3-ethyl-2-thioxo-4- thiazolidinone (**5**) [20], 2,3-dimethylbenzothiazolium iodide (**7**) [21,22], 1,4-dimethylquinolinium iodide (**8**) [21,22] were prepared according to the literatures with some modification.

2.2.1. 2-Methylthiobenzothiazole (**2**)

The 2-mercaptobenzothiazole (**1**; 3.01 g, 18.0 mmol) was dissolved in 7.5 mL of 10% NaOH, and dimethyl sulfate (1.7 mL, 18.0 mmol) was added dropwise under stirring at 40 °C, the resulting mixture was stirred at 40 °C for 0.5 h. After the reaction mixture was cooled to room temperature and extracted with ether, and the organic phase was dried over anhydrous magnesium sulfate, filtered and evaporated off ether to give (**2**) (2.17 g, yield 66.6%) as white crystals, m.p. 51–52 °C (lit, m.p. 52 °C).

2.2.2. 3-Methyl-2-methylthiobenzothiazolium iodide (**3**)

A mixture of 2-methylthiobenzothiazole (**2**; 2.17 g, 12.0 mmol) and methyl iodide (2.84 g, 20.0 mmol) in methanol was stirred at 43 °C for 24 h. After cooling, excess methyl iodide and methanol were evaporated and the product was washed with ether to give (**3**) (2.80 g, 72.2%) as colorless crystals, m.p. 142–143 °C (lit, m.p. 146 °C).

2.2.3. 5-(3-Methyl-(3H)-benzothiazol-2-ylidene)-3-ethyl-2-thioxo-4-thiazolidinone (**5**)

A mixture of 3-methyl-2-methylthiobenzothiazolium iodide (**3**; 1.29 g, 4.0 mmol), 3-ethylrhodanine (**4**; 0.65 g, 4.0 mmol) and a few drops of triethylamine in ethanol was refluxed for 3 h. After cooling, the product was filtered to give (**5**) (1.20 g, 97.6%) as yellow powder, m.p. 260–264 °C (lit, m.p. 265 °C).

2.2.4. 2,3-Dimethylbenzothiazolium iodide (**7**)

A mixture of 2-methylbenzothiazole (5.07 g, 34.0 mmol) and methyl iodide (5.00 g, 35.2 mmol) in ethanol was stirred at room temperature for 0.5 h, then the mixture was heated to reflux for 24 h. After cooling, the product was filtered to give (**7**) (8.75 g, 88.4%) as white powder, m.p. 218–220 °C (lit, m.p. 221–222 °C).

2.2.5. 1,4-Dimethylquinolinium iodide (**8**)

A mixture of 4-methylquinoline (2.86 g, 20 mmol) and methyl iodide (4.26 g, 30 mmol) in ethanol was stirred at room temperature for 0.5 h, then the mixture was heated to reflux for 12 h. After the reaction mixture was cooled to room temperature, the product was filtered to give (**8**) (3.80 g, 66.7%) as yellow crystals, m.p. 176–177 °C (lit, m.p. 174–175 °C).

2.3. Preparation of the intermediate **6** and two dyes **9a**, **9b**

2.3.1. Preparation of dye **9a**

A mixture of (**5**) (0.31 g, 1.0 mmol) and methyl *p*-toluenesulfonate (0.52 g, 3.0 mmol) in *N*,*N*-dimethylformamide (10.0 mL) was stirred at 130 °C for 2.5 h. After the mixture was cooled to room temperature, ether (30 mL) was added and the product was filtered to give yellow solid (**6**).

The obtained compound (**6**) was dissolved in 5.0 mL acetonitrile, and 2,3-dimethylbenzothiazolium iodide (**7**; 0.29 g, 1.0 mmol) was then added, followed by a few drops of triethylamine. And the

mixture was stirred at 70 °C for 1 h. After cooling, the precipitate was collected and washed with acetonitrile and ethylacetate respectively. Then the product was purified with methanol by Soxhlet extraction in 48 h to give **9a** (0.12 g, 21.1%, two steps).

2.3.2. Preparation of dye *9b*

A mixture of (**5**) (0.37 g, 1.2 mmol) and methyl *p*-toluenesulfonate (0.62 g, 3.6 mmol) in *N*,*N*-dimethylformamide (10.0 mL) was stirred at 130 °C for 2.5 h. After the mixture was cooled to room temperature, ether (30 mL) was added and the product was filtered to give yellow solid (**6**).

The obtained compound (**6**) was dissolved in 5.0 mL acetonitrile, 1,4-dimethylquinolinium iodide (**8**; 0.34 g, 1.2 mmol) was then added, followed by a few drops of triethylamine. And the mixture was stirred at 70 °C for 1 h. After cooling, the precipitate was collected and washed with acetonitrile and ethylacetate respectively. Then the product was purified with methanol by Soxhlet extraction in 48 h to give **9b** (0.23 g, 34.3%, two steps).

2.4. Structural confirmation

2.4.1. 2-[3-Ethyl-5-(3-methyl-(3H)-benzothiazol-2-ylidene)-4-oxothiazolidin-2-ylidenemethyl]-3-methyl benzothiazolium iodide (*9a*)

Orange-red crystals, m.p.: 248–249 °C. ^{1}H NMR (400 MHz, DMSO-d_6) δ(ppm): 1.30 (t, J = 6.4 Hz, 3H, $-CH_3$), 4.08 (s, 3H, N$-CH_3$), 4.23 (s, 3H, N^+-CH_3), 4.28 (b, 2H, $-CH_2-$), 6.71 (s, 1H, $-CH=$), 7.38 (d, J = 7.2 Hz, 1H, ArH), 7.55 (d, J = 7.2 Hz, 2H, ArH), 7.73 (d, J = 7.2 Hz, 2H, ArH), 7.95–8.01 (m, 2H, ArH), 8.26 (d, J = 7.2 Hz, 1H, ArH); IR (KBr, cm^{-1}): 3020 (w, $\upsilon_{=C-H}$), 2930 (w, υ_{C-H}), 1648 (s, $\upsilon_{C=O}$), 1539 (s, $\upsilon_{C=C}$, $\upsilon_{C=N}$), 1494 (s, δ_{CH}), 1317 (s, υ_{C-N}), 1268, 1200, 1065 (s, υ_{C-N}, δ_{CH}), 748 (s, $\delta_{=C-H}$); MS (70 eV) *m*/*z* (%): 423 (M$-ICH_3-CH_3$, 100), 379 (M$-ICH_3-CH_3-C_2H_5$, 5), 368 (M$-ICH_3$ $-CH_3-C_2H_5-$O, 45), 289 (M$-ICH_3-C_8H_7$NS, 49); HRMS (TOF MS ES-) calculated for $C_{22}H_{20}N_3OS_3^+$: 438.0763, found: 438.0769; UV–Vis (MeOH) λ_{max}: 500.0 nm.

2.4.2. 4-[3-Ethyl-5-(3-methyl-(3H)-benzothiazol-2-ylidene)-4-oxothiazolidin-2-ylidenemethyl]-1-methyl quinolinium iodide (*9b*)

Darkviolet crystals, m.p. >298 °C. ^{1}H NMR (400 MHz, DMSO-d_6) δ (ppm): 1.30 (t, J = 6.4 Hz, 3H, $-CH_3$), 4.17 (s, 3H, N$-CH_3$), 4.28 (s, 3H, N^+-CH_3), 4.32 (b, 2H, $-CH_2-$), 6.94 (s, 1H, $-CH=$), 7.35 (t, J = 7.7 Hz, 1H, ArH), 7.54 (t, J = 7.7 Hz, 1H, ArH), 7.63 (d, J = 7.6 Hz, 1H, ArH), 7.72 (d, J = 8.0 Hz, 1H, ArH), 7.85 (t, J = 7.7 Hz, 1H, ArH), 7.94 (d, J = 8.4 Hz, 1H, ArH), 8.03 (t, J = 7.6 Hz, 1H, ArH), 8.17 (d, J = 8.0 Hz, 1H, ArH), 8.72 (d, J = 6.4 Hz, 1H, ArH), 8.81 (d, J = 8.8 Hz, ArH); IR (KBr, cm^{-1}): 3015 (w, $\upsilon_{=C-H}$), 2966 (w, υ_{C-H}), 1636 (s, $\upsilon_{C=O}$), 1539 (s, $\upsilon_{C=C}$, $\upsilon_{C=N}$), 1494 (s, δ_{CH}), 1315 (s, υ_{C-N}), 1228, 1200, 1071 (s, υ_{C-N}, δ_{CH}), 750 (s, $\delta_{=C-H}$); MS (70 eV) *m*/*z* (%): 359 (M$-ICH_3-CH_3-C_2H_5-$O, 5), 275 (M$-ICH_3-CH_3-C_9H_6$N, 48); 268 (M$-ICH_3-CH_3-C_7H_5$NS, 50), 246 (M$-ICH_3-CH_2CH_3-C_{10}H_{10}$, 100); HRMS (TOF MS ES-) calculated for $C_{24}H_{22}N_3OS_2^+$: 432.1199, found: 432.1205; UV–Vis (MeOH) λ_{max}: 566.0 nm.

2.5. Measurements of the spectral properties of the dyes in different solvents

The dye stock solutions (5.0 × 10^{-3} mol L^{-1} in DMSO) were diluted with different solvents and resulted in working solutions of dyes (5.0 × 10^{-5} mol L^{-1}). The absorption spectra were examined at room temperature in different solvents and recorded using 1 cm quartz cells on a Purkinje General UV-1900 UV–Vis spectrometer. Fluorescence measurements were carried out at room temperature on a Hitachi F-4500 spectrofluorimeter in 1 cm quartz cells. Fluorescence emission was excited at the maximum of the absorption. The absorption and fluorescence spectral data were listed in Table 1.

Table 1
The physical constant and the spectral data of dye **9a**, **9b** in different solvents.

Dye	Solvent	Permittivity	Refractive index	λ_{max}/nm	λ_{em}/nm	Stockes shift/nm	$\varepsilon \times 10^{-4}$/ M^{-1} cm^{-1}
9a	H_2O	78.5	1.3325	471.0	574.0	103.0	6.2
	MeOH	32.6	1.3290	501.0	559.0	58.0	8.3
	EtOH	24.3	1.3614	503.0	559.0	56.0	8.0
	DMSO	47.2	1.4780	506.0	565.0	59.0	8.1
	DMF	36.7	1.4304	503.0	565.0	62.0	7.5
	MeCOMe	20.5	1.3587	501.0	564.0	63.0	8.0
9b	H_2O	78.5	1.3325	520.0	658.0	138.0	4.1
	MeOH	32.6	1.3290	567.0	–	–	5.8
	EtOH	24.3	1.3614	569.0	625.0	56.0	5.7
	DMSO	47.2	1.4780	571.0	647.0	76.0	5.8
	DMF	36.7	1.4304	569.0	–	–	5.3
	MeCOMe	20.5	1.3587	568.0	–	–	5.6

2.6. Measurements of spectral properties of the dyes in the presence of DNA or BSA

Dyes stock solutions (5.0 × 10^{-3} mol L^{-1}) were prepared by dissolving the dyes in DMSO and further diluted with TE buffer (10 mmol L^{-1} Tris–HCl, 1 mmol L^{-1} EDTA, pH 7.5) to result in working solutions of dyes (1.0 × 10^{-6} mol L^{-1}). Stock solutions of DNA or BSA were prepared by dissolving DNA or BSA in TE buffer. The concentrations of DNA or BSA in stock solutions were 8 × 10^{-5} mol L^{-1} base pairs (bp) for DNA and 0.5 mg mL^{-1} for BSA. Working solutions of complexes DNA-dyes and BSA-dyes were prepared by mixing an aliquot of dyes stock solutions and an aliquot of DNA or BSA stock solutions, and further diluted with TE buffer to obtain 1.6 × 10^{-5} mol L^{-1} bp for DNA-dyes or 0.1 mg mL^{-1} for BSA-dyes. All working solutions were prepared immediately before the experiment. Measurements method was mentioned as above. The absorption and fluorescence spectral data were listed in Table 2, Table 3 and Fig. 1.

2.7. Study on K562 cells

2.7.1. Cell culture and treatment with the dyes

K562 cells were cultured in RPMI 1640 medium supplemented with 10% (v/v) newborn calf serum, 1% (v/v) L-glutamine and 100 units/mL antibiotics (penicillin and streptomycin) at 37 °C and 5% CO_2 humidified incubator. The dyes were dissolved in DMSO and stored at −20 °C at a concentration of 1 mM. For the cell growth assay, cells were seeded into 6-well plates at a density of 1 × 10^5 cells/mL and treated with the dyes or with DMSO only (as control). The final concentration of DMSO was kept at less than 0.05%. K562 cells were incubated with the dyes for 4 h at 37 °C before PDT irradiation.

2.7.2. Photodynamic treatment

Photodynamic treatment was performed according to the literature [23]. K562 cells in the exponential phase of growth were harvested and suspended in RPMI 1640 medium at a density of

Table 2
Spectral characteristics of dye **9a**, **9b** in buffer.

Dye	In buffer				
	λ_{max}/nm	ε^{free} (M^{-1} cm^{-1})	λ_{ex}/nm	λ_{em}/nm	Φ_F^{free}
9a	500.0	1.2 × 10^4	500.0	566.8	0.0025
9b	563.0	6.0 × 10^3	563.0	–	–

Table 3
Spectral characteristics of dye **9a**, **9b** in DNA or BSA presence.

Dye	λ_{max}/nm	ε^{DNA} (M^{-1} cm^{-1})	λ_{ex}/nm	λ_{em}/nm	Φ_F^{DNA}	$\Phi_F^{DNA}/\Phi_F^{free}$
In DNA presence						
9a	504.0	3.2×10^4	480.0	550.0	0.0738	29.52
9b	569.0	1.3×10^4	550.0	642.0	0.0020	–
	λ_{max}/nm	ε^{BSA}(M^{-1} cm^{-1})	λ_{ex}/nm	λ_{em}/nm	Φ_F^{BSA}	$\Phi_F^{BSA}/\Phi_F^{free}$
In BSA presence						
9a	495.0	1.5×10^4	495.0	560.8	0.0027	1.08
9b	564.0	7.0×10^3	564.0	–	–	–

1×10^5 cells/mL. The cells were incubated for 4 h with 1 mM the dyes at 37 °C. Afterward the cells were seeded in 6-well plates. The cells were illuminated with a light intensity of 350 mW/cm^2 and light doses of 105 J/cm^2. The radiation source was a xenon lamp emitting wavelengths over the range 400–800 nm.

2.7.3. Measurement of cell viability

The effect of the dyes on growth of K562 cells was determined by hemacytometer. K562 cells were seeded into 6-well plates at a density of 1×10^5 cells/mL and incubated at 37 °C in 5% CO_2. After experiments, the cells were stained by 0.2% trypan blue and then counted with a hemacytometer. The percent of inhibition cell proliferation and cell survival was calculated as follows: % Survival = (survival/control) × 100%. All experiments were performed in triplicates. Data were expressed as mean + SD. Experimental results were listed in Fig. 2.

3. Results and discussion

3.1. Synthesis of dyes

The rhodanine complex merocyanine dyes **9a** and **9b** were synthesized via the reaction of intermediate compound (**6**) with 2,3-dimethylbenzothiazole quaternary salt (**7**) or 1,4-dimethylquinolinequaternary salt (**8**) (Scheme 1). The intermediate compound (**6**) was easily obtained by S-methylation and N-methyl quaternization of 2-mercaptobenzothiazole (**1**), the condensation of 3-methyl-2-methylthiobenzothiazolium iodide (**3**) with 3-ethylrhodanine (**4**) in the presence of triethylamine, and methylating the thiocarbonyl group of the 5-(3-methyl-(3H)-benzothiazol-2-ylidene)-3-ethyl-2-thioxo-4-thiazolidinone (**5**), successively. The intermediate compound (**7**) or (**8**) were prepared by N-methyl quaternization of 2-methylbenzothiazole or 4-methylquinoline. In all cases investigated, we found that two rhodanine complex merocyanine dyes could be purified by soxhlet extraction with methanol. And intermediate 5-(3-methyl-(3H)-benzothiazol-2-ylidene)-3-ethyl-2-thioxo-4-thiazolidinone (**5**) was introduced into the following reaction of synthesizing rhodanine complex merocyanine dye **9a**, **9b** without purification. The dyes with higher purity could be obtained, and the procedure was simplified as well.

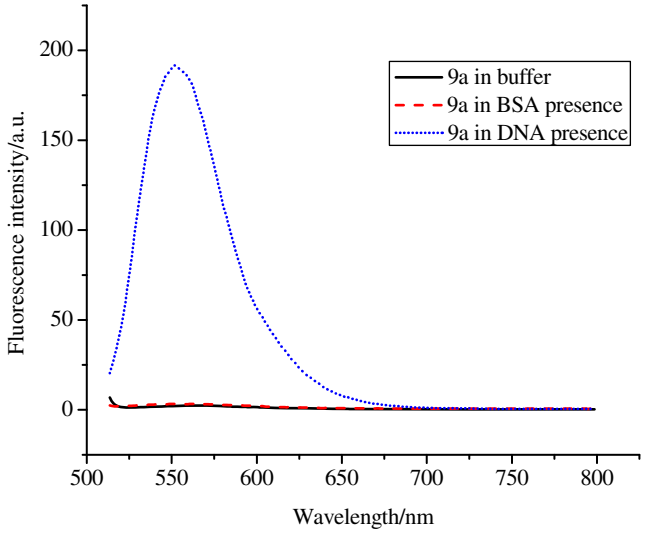

Fig. 1. Fluorescence spectra of dye **9a** in buffer and in the presence of DNA or BSA.

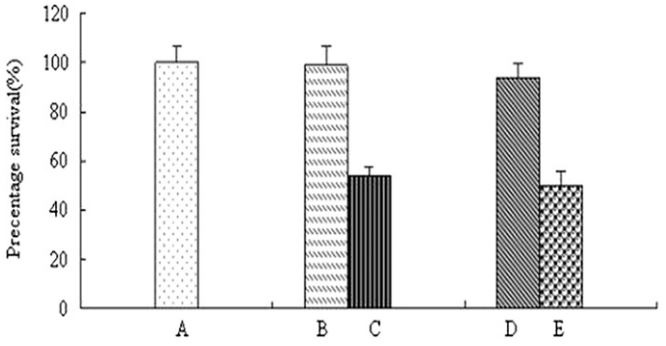

Fig. 2. Effects of dyes **9a** and **9b** on cell survival A. Cell survival rate treated with DMSO only (as control) without dyes; B and D. Cell survival rate treated with dyes **9a** and **9b**, respectively; C and E. Cell survival rate treated with dyes **9a** and **9b** respectively and PDT irradiation.

3.2. E,Z geometry of two dyes and DFT calculations

Because of C=C double bonds, there are four geometric isomers in dyes **9a** and **9b**, respectively. The configurations and energies of the geometric isomers are carried out at B3LYP/6-31G* level according to the literature [24], and their optimized configurations and energies are given in Fig. 3 and Fig. 4. It can be found that the isomers II and II′ is of a minimum single point energy for dye **9a** and for dye **9b**, respectively. Therefore isomer II is the most stable form in all isomers for dye **9a**, and isomer II′ is the most stable form in all isomers for dye **9b**. So the geometry of dyes **9a** and **9b** is isomers II and II′ respectively, which is consistent with the literature [12]. Dyes reported in the literature are complex merocyanine dyes, which are similar to the dyes we synthesize in this work.

3.3. Spectral properties of the dyes in different solvents

Table 1 gives the spectral properties of the dyes in different solvents. From Table 1, it could be found that the shortest λ_{max} of dye **9a** or **9b** was in water. The reason was that the hydrogen bonds created between water molecules in aqueous medium and dye molecules could reduce the delocalization of the lone pair of electrons of hetrocyclic nitrogen, which lead to the observed solvatochromic behavior [25]. It could be also found that the λ_{max} of the dyes exhibited hypsochromic shifts with the increase of the polarity of the solvent in protonic solvents (Permittivity: EtOH 24.3, MeOH 32.6, H_2O 78.5), that is λ_{max} (EtOH) > λ_{max} (MeOH) > λ_{max} (H_2O). The effect could be illustrated by hydrogen-bonding interaction between the protonic solvents and the dye molecules, which made the ground state energy of dyes decrease, and consequently increased the transition energy of dye molecules [26]. The greater the polarity of protonic solvents was, and the smaller the size of protonic solvents was, the greater was hydrogen-bonding interaction between the protonic solvents and the dye molecules. It could be also found that the λ_{max} of the dyes exhibited bathochromic

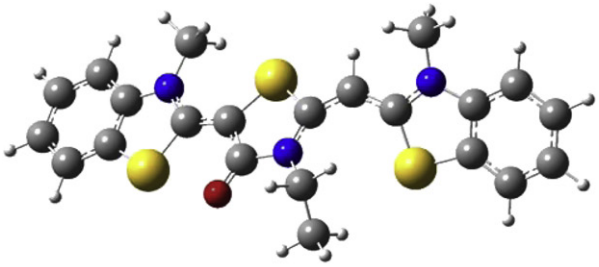

HF (hartree): -2284.2477438 I

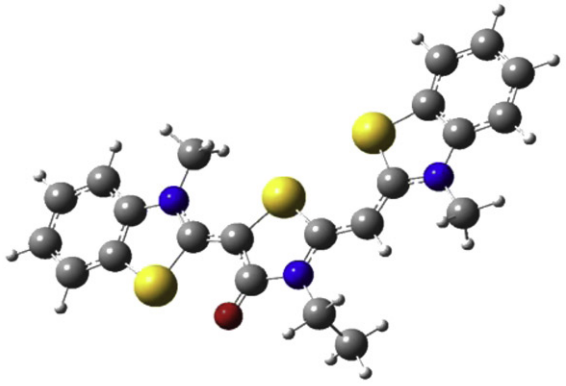

HF (hartree): -2284.2602522 II

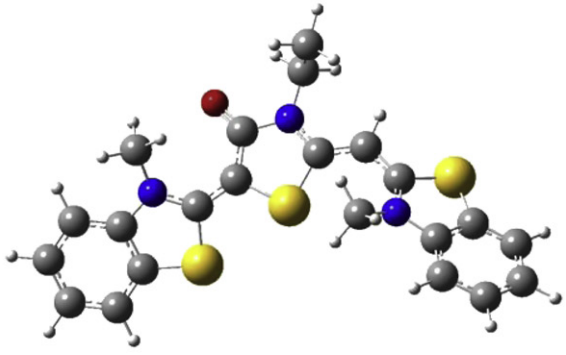

HF (hartree): -2284.2476723 III

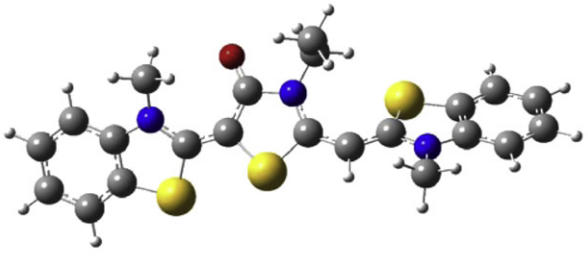

HF (hartree): -2284.2405986 IV

Fig. 3. The optimized configurations and energies of four geometric isomers for dye **9a**.

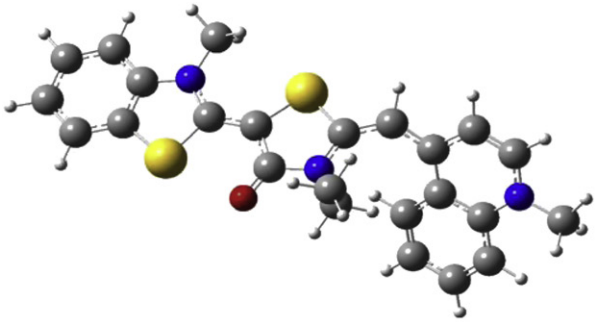

HF (hartree): -1963.4787471 I'

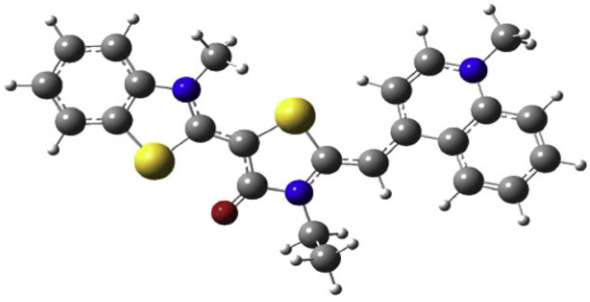

HF (hartree): -1963.4908010 II'

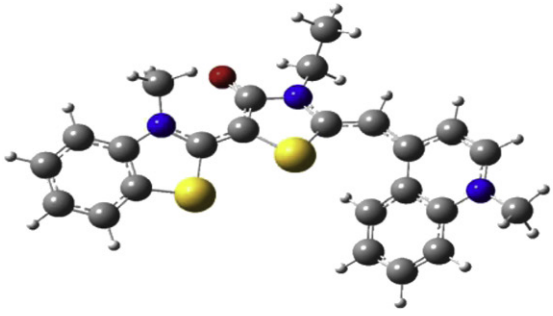

HF (hartree): -1963.4806963 III'

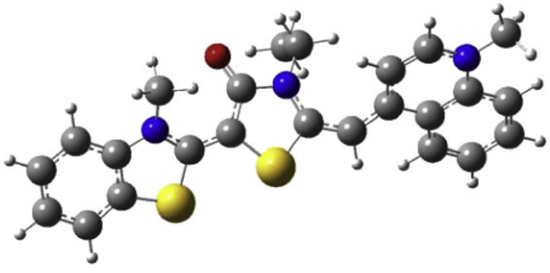

HF (hartree): -1963.4803705 IV'

Fig. 4. The optimized configurations and energies of four geometric isomers for dye **9b**.

shifts with the increase of refractive index in non protonic solvent, that is λ_{max} (DMSO) > λ_{max} (DMF) > λ_{max} (MeCOMe); The Stokes shift of two dyes in water were relatively large, which could help to reduce self-quenching and measurement error by excitation light and scattered light [27,28].

3.4. Spectral properties of the dyes in the presence of DNA or BSA

The detailed spectral properties of the dyes **9a** and **9b**, DNA-dyes and BSA-dyes were measured in buffer (Table 2 and Table 3). From Table 2 and Table 3, it could be found that absorption maxima of

Table 4
The selected dihedral angles (°) of dyes **9a** and **9b**.

Dyes	D(1,3,4,5)[a]	D(1,3,4,6)[a]	D(2,3,4,5)[a]	D(2,3,4,6)[a]	D(5,8,9,10)[a]	D(5,8,9,11)[a]	D(7,8,9,10)[a]	D(7,8,9,11)[a]
9a	−7.39	178.42	172.05	−2.13	1.01	−178.62	−178.58	1.78
9b	−7.49	178.15	172.03	−2.33	−11.63	168.34	172.51	−7.55

[a] The atom labels are marked in Scheme 1.

DNA-dye **9a**, **9b** and BSA-dye **9b** showed a slight red shift, which were situated at 504.0, 569.0 and 564.0 nm, relative to the corresponding maxima of free dyes in buffer, but BSA-dye **9a** was an exception. The molar extinction coefficients for two dyes were all increased in the presence of DNA or BSA.

From Table 2, it could also be found that dye **9a** showed better fluorescent performance than dye **9b**. The reason was that the compound could emit fluorescence was closely related to the molecular structure (The selected dihedral angles (°) of dyes **9a** and **9b** were shown in Table 4), the better planar structural rigidity and the larger π conjugated system of the molecular was, the stronger fluorescence it appeared [29]. The emission maxima of DNA-dye **9a** and BSA-dye **9a** were located at 550.0, 560.8 nm and showed a slight blue shift relative to free dye **9a** in buffer. Fig. 1 showed that fluorescence intensity of dye **9a** was greatly increased in the presence of DNA. Compared with free dye **9a**, the quantum yields of DNA-dye **9a** was up to 29.52 times. It was noteworthy that free dye **9b** could not be detected significantly fluorescence in buffer, and displayed slight fluorescence in the presence of DNA, and BSA-dye **9b** in buffer could not be detected significantly fluorescence. The fluorescence enhancement of dyes in the presence of DNA was attributable to the fact that on photoexcitation a lack of free rotation around the internuclear bridge made isomerization around the C–C bonds of the methine chain difficult, and subsequently nonradiative deactivation of the excited state was not possible, causing the dye to fluoresce [30].

3.5. Influence of two dyes on K562 cells survivaln

Using dye **9a** or **9b** as photosensitizers for PDT analyzed its effect on K562 cells survival, as shown in Fig. 2. It could be found that the viable cells were incubated for 4 h with 1 mM dye **9a** or **9b** at 37 °C in the cultures, they almost had no effect on the cells growth compared with control group (Sur_A:Sur_B:Sur_D = 100%:99%:94%). The viable cells were greatly reduced when incubating and irradiating in the presence of dye **9a** or **9b** (Sur_B:Sur_C = 99%:56%; Sur_D:Sur_E = 94%:50%). These data confirmed that supplementation of dye **9a** or **9b** as photosensitizers for PDT in K562 cells decreases the survival rate. It was suggested that this kind of dyes (**9a**, **9b**) had DLC (π-delocalized lipophilic cation) effects, which had selective uptake and retention by mitochondria of K562 cells to kill it [11,17].

4. Conclusions

Two rhodanine complex merocyanine dyes **9a** and **9b** were synthesized and the products were identified by ^{1}H NMR, IR, MS, HRMS, UV–Vis, then tested in concerned experiments, such as spectrum, photodynamic therapy etc. The λ_{max} of two dyes showed hypsochromic shifts with the increase of permittivity in protonic solvents, and bathochromic shifts with the increase of refractive index in non protonic solvent. The quantum yield of DNA-dye **9a** was up to 29.5 times compared with free dye **9a**. Supplementation of dye **9a** or **9b** as photosensitizers for PDT in K562 cells decreases the survival rate.

Acknowledgment

We appreciate the financial support for this research by a grant from the Special Science Research Foundation of Education Committee (No. 11JK0558), the Natural Science Foundation of Shaanxi Province (No. SJ08B04), Key Scientific Research Base open funds of NWU (ZS11013), NWU Graduate Cross-discipline Funds (No. 09YJC20), NWU Excellent Doctoral Dissertation Foundation (No. 08YYB04).

References

[1] Schmitt F, Govindaswamy P, Georg SF, Wee HA, Dyson Paul J, Lucienne JJ, et al. Ruthenium porphyrin compounds for photodynamic therapy of cancer. J Med Chem 2008;51(6):1811–6.
[2] Sharman WM, van Lier JE, Allen CM. Targeted photodynamic therapy via receptor mediated delivery systems. Adv Drug Deliver Rev 2004;56(1):53–76.
[3] Sol V, Chaleix V, Champavier Y, Granet R, Huang YM, Krausz P. Glycosyl bisporphyrin conjugates: synthesis and potential application in PDT. Bioorgan Med Chem 2006;14(23):7745–60.
[4] Gorman SA, Bell AL, Griffiths J, Roberts D, Brown SB. The synthesis and properties of unsymmetrical 3,7-diaminophenothiazin-5-ium iodide salts: potential photosensitisers for photodynamic therapy. Dyes Pigm 2006;71(2):153–60.
[5] Chen YH, William RP, Joseph RM, Morgan J, Ravindra KP. Comparative in vitro and in vivo studies on long-wavelength photosensitizers derived from bacteriopurpurinimide and bacteriochlorin p_6: fused imide ring enhances the in vivo PDT efficacy. Bioconjug Chem 2007;18(5):1460–73.
[6] Davids LM, Kleemann B. Combating melanoma: the use of photodynamic therapy as a novel, adjuvant therapeutic tool. Cancer Treat Rev 2011;37(6):465–75.
[7] Jiang XJ, Yeung SL, Lo PC, Fong WP, Ng DK. Phthalocyanine–polyamine conjugates as highly efficient photosensitizers for photodynamic therapy. J Med Chem 2011;54(1):320–30.
[8] Renikuntla BR, Rose HC, Eldo J, Waggoner AS, Armitage BA. Improved photostability and fluorescence properties through polyfluorination of a cyanine dye. Org Lett 2004;6(6):909–12.
[9] Deligeorgiev TG, Gadjev NI, Vasilev AA, Maximova VA, Timcheva II, Katerinopoulos HE, et al. Synthesis and properties of novel asymmetric monomethine cyanine dyes as non-covalent labels for nucleic acids. Dyes Pigm 2007;75(2):466–73.
[10] Zhang XH, Wang LY, Nan ZX, Tan SH, Zhang ZX. Microwave-assisted solvent-free synthesis and spectral properties of some dimethine cyanine dyes as fluorescent dyes for DNA detection. Dyes Pigm 2008;79(2):205–9.
[11] Sun XC, Wong JR, Song K, Hu JL, Garlid KD, Chen LB. AA1, A newly synthesized monovalent lipophilic cation, expresses potent in vivo antitumor activity. Cancer Res 1994;54(6):1465–71.
[12] Kawakami M, Koya K, Ukai T, Tatsuta N, Ikegawa A, Ogawa K, et al. Structure-activity of novel rhodacyanine dyes as antitumor agents. J Med Chem 1998; 41(1):130–42.
[13] Takasu K, Inoue H, Kim HS, Suzuki M, Shishido T, Wataya Y, et al. Rhodacyanine dyes as antimalarials. 1. Preliminary evaluation of their activityand toxicity. J Med Chem 2002;45(5):995–8.
[14] Takasu K, Terauchi H, Inoue H, Kim HS, Wataya Y, Ihara M. Parallel synthesis of antimalarial rhodacyanine dyes by the combination of three components in one pot. J Comb Chem 2003;5(3):211–4.
[15] Takasu K, Terauchi H, Inoue H, Takahashi M, Sekita S, Ihara M. Antileishmanlal activities of rhodacyanine dyes. Heterocycles 2004;64:215–21.
[16] Takasu K, Pudhom K, Kaiser M, Brun R, Ihara M. Synthesis and antimalarial efficacy of aza-fused rhodacyanines in vitro and in the *P. berghei* mouse model. J Med Chem 2006;49(15):4795–8.
[17] Pudhom K, Kasai K, Terauchi H, Inoue H, Kaiser M, Brun R, et al. Synthesis of three classes of rhodacyanine dyes and evaluation of their in vitro and in vivo antimalarial activity. Bioorgan Med Chem 2006;14(24):8550–63.
[18] Ivan Heilbron. Dictionary of organic compounds I. Beijing: Science Press; 1964 [in Chinese].
[19] Kendall JD, Suggate HG. Reactivity of the alkylmercapto group in nitrogen ring compounds. I. A general method for the preparation of symmetrical and unsymmetrical thiacyanines. J Chem Soc; 1949:1503–9.
[20] Liu Q, Wang X, Wang LY, Fu YL, Zhang XH. The synthesis, spectroscopic properties and crystal structures of some rhodanine merocyanine dyes for optical recording with a blue diode laser. Dyes Pigm 2011;91(3):370–7.
[21] Kiprianov AI, Rozum YS. Ultraviolet absorption spectra of benzothiazole derivatrives. Zh Obshch Khim 1951;21:2038–45.

[22] Leonard NJ, DeWalt HAJ, Leubner GW. Reactions of quinolinium compounds with nitromethane. J Am Chem Soc 1951;73(7):3325–9.
[23] Sun D, Zhang SJ, Wei YF, Yin LF. Antioxidant activity of mangostin in cell-free system and its effect on K562 leukemia cell line in photodynamic therapy. Acta Biochim Biophys Sin 2009;41(12):1033–43.
[24] Zhang XH, Wang LY, Zhan YH, Fu YL, Zhai GH, Wen ZY. Synthesis and structural studies of 4-[(5-methoxy-1H-indole-3-yl)-methylene]-3-methyl-isoxazole-5-one by X-ray crystallography, NMR spectroscopy, and DFT calculations. J Mol Struct 2011;994(1–3):371–8.
[25] El-Shishtawy RM, Asiri AM, Basaif SA, Sobahi TR. Synthesis of a new β-naphthothiazole monomethine cyanine dye for the detection of DNA in aqueous solution. Spectrochim Acta A 2010;75(5):1605–9.
[26] Pham W, Lai WF, Weissleder R, Tung CH. High efficiency synthesis of a bioconjugatable near-infrared fluorochrome. Bioconjug Chem 2003;14(5):1048–51.
[27] Tolosa L, Nowaczyk K, Lakowicz J. An introduction to laser spectroscopy. 2nd ed. New York: Kluwer; 2002.
[28] Zhang ZR, Achilefu S. Synthesis and evaluation of polyhydroxylated near-infrared carbocyanine molecular probes. Org Lett 2004;6(12):2067–70.
[29] Cheng GZ, Huang XZ, Zheng ZZ, Xu JG, Wang ZB. The analytical method of fluorescence. 2nd ed. Beijing: Science Press; 1990.
[30] Anikovsky MY, Tatikolov AS, Shvedove LA, Kuzmin VA. Photochemical investigation of the triplet state of 3,3'-diethylthiacarbocyanine iodide in the presence of DNA. Russ Chem Bull 2001;50(7):1190–3.